Improvement of $^4I_{11/2} \rightarrow {}^4I_{13/2}$ Transition Rate and Thermal Stabilities in Er^{3+}-Doped TeO_2-B_2O_3 (GeO_2)-ZnO-K_2O Glasses

Doo Hee Cho, Yong Gyu Choi, and Kyong Hon Kim

Spectroscopic and thermal analysis indicates that tellurite glasses doped with B_2O_3 and GeO_2 are promising candidate host materials for wide-band erbium doped fiber amplifier (EDFA) with a high 980 nm pump efficiency. In this study, we measured the thermal stabilities and the emission cross-sections for Er^{3+}: $^4I_{13/2} \rightarrow {}^4I_{15/2}$ transition in this tellurite glass system. We also determined the Judd-Ofelt parameters and calculated the radiative transition rates and the multiphonon relaxation rates in this glass system. The 15 mol% substitution of B_2O_3 for TeO_2 in the Er^{3+}-doped $75TeO_2$-$20ZnO$-$5K_2O$ glass raised the multiphonon relaxation rate for $^4I_{11/2} \rightarrow {}^4I_{13/2}$ transition from 4960 s^{-1} to 24700 s^{-1}, but shortened the lifetime of the $^4I_{13/2}$ level by 14 % and reduced the emission cross-section for the $^4I_{13/2} \rightarrow {}^4I_{15/2}$ transition by 11%. The 15 mol% GeO_2 substitution in the same glass system also reduced the emission cross-section but increased the lifetime by 7%. However, the multiphonon relaxation rate for $^4I_{11/2} \rightarrow {}^4I_{13/2}$ transition was raised merely by 1000 s^{-1}. Therefore, a mixed substitution of B_2O_3 and GeO_2 for TeO_2 was concluded to be suitable for the 980 nm pump efficiency and the fluorescence efficiency of $^4I_{13/2} \rightarrow {}^4I_{15/2}$ transition in Er^{3+}-doped tellurite glasses.

I. INTRODUCTION

A tellurite-based erbium doped fiber amplifier (T-EDFA) provides a wide amplifying bandwidth due to its high stimulated emission cross-section [1], [2]. T-EDFA shows a broad bandwidth of over 70 nm with a medium population inversion in contrast to a silica-based EDFA that shows about a 30 nm bandwidth. The EDFA for amplification of 1.5 µm signal can use both 980 nm and 1480 nm optical pumping. Generally, the 1480 nm pumping is suitable for high power EDFA because the ground state absorption to $^4I_{13/2}$ manifold has a high absorption cross-section relative to that of $^4I_{11/2}$. However, the 1480 nm pumping is a resonant pumping scheme that cannot provide full population inversion and good signal-to-noise ratio (S/N)[3]. Thus, the 980 nm pumping scheme on T-EDFA is necessary for the wide bandwidth optical amplifier with a good noise figure. It has been reported that the small signal gain of T-EDFA with 980 nm pumping is significantly lower than that with 1480 nm pumping [4]. This may be due to the low phonon energy of tellurite glasses. For Er^{3+} doped in silicate glasses, the lifetime of $^4I_{11/2}$ is less than 10 µs due to the high multiphonon relaxation rate, and population feeding from $^4I_{11/2}$ to $^4I_{13/2}$ results dominantly from the multiphonon relaxation [5]. The highest phonon energy of silicate glasses is around 1100 cm^{-1}, while that of tellurite glasses is around 700cm^{-1} [6]. Therefore, the multiphonon relaxation rate of the $^4I_{11/2} \rightarrow {}^4I_{13/2}$ transition of Er^{3+} in tellurite glasses is much smaller than that in silicate glasses, and the lifetime of $^4I_{11/2}$ for tellurite glasses is much longer than that for silicate glasses. This results in several undesirable effects on the 980 nm pumping efficiency in Er^{3+}-doped tellurite glasses. First, the accumulation of population in the

$^4I_{13/2}$ level becomes difficult because the branching ratio of the radiative $^4I_{11/2} \rightarrow {}^4I_{13/2}$ transition is about four times smaller than that of the $^4I_{11/2} \rightarrow {}^4I_{15/2}$ transition [7]. Secondly, the cross relaxation of $^4I_{11/2} : {}^4I_{11/2} \rightarrow {}^4F_{7/2} : {}^4I_{15/2}$ may depopulate the $^4I_{11/2}$ level. Finally, excited state absorption of $^4I_{11/2} \rightarrow {}^4F_{7/2}$ by the pumping light can also depopulate the $^4I_{11/2}$ level [8]. Consequently, the improvement in the multiphonon relaxation rate of $^4I_{11/2} \rightarrow {}^4I_{13/2}$ in Er^{3+}-doped tellurite glasses can enhance the population accumulation in the $^4I_{13/2}$ level and the 980 nm pumping efficiency. We have already proposed that the Ce^{3+}-codoping can enhance the 980 nm pumping efficiency through the non-radiative energy transfer $Er^{3+} : {}^4I_{11/2}, Ce^{3+} : {}^2F_{5/2} \rightarrow Er^{3+} : {}^4I_{13/2}, Ce^{3+} : {}^2F_{7/2}$ [9]. In this study, we propose another effective method to increase the 980 nm pumping efficiency. The addition of B_2O_3 along with GeO_2 into Er^{3+}-doped tellurite glasses is considered to increase the highest phonon energy of host glasses and the multiphonon relaxation rate of the $^4I_{11/2} \rightarrow {}^4I_{13/2}$ transition, and then successfully to enhance the population accumulation in the $^4I_{13/2}$ level and the 980 nm pumping efficiency.

II. EXPERIMENTAL

Glass samples were prepared by a conventional melting and quenching method. Starting materials were oxide and carbonate powders with more than 99.9% purity. Melting was carried out in air by using an electric furnace. Mixed powder was melted in an alumina crucible at 950°C for 60 minutes, and cast on a brass plate preheated at about 200°C, then annealed at 380°C for 20 minutes. Glass transition and crystallization temperatures were measured by differential scanning calorimetry (DSC) thermal analysis. A Ti: sapphire laser excited by Ar ion laser was used to pump the sample, and a monochromator and an InGaAs detector were used to measure the fluorescence spectrum. The fluorescence lifetimes for the $^4I_{11/2}$ and $^4I_{13/2}$ levels were measured with a Ti: sapphire laser, a chopper wheel, and the optical detector coupled with a HP 500 MHz digital oscilloscope. The wavelength of the excitation laser was tuned to 800 nm for the fluorescence spectrum and lifetime measurements. Absorption spectra were measured with a UV-Visible-NIR spectrophotometer.

III. RESULTS AND DISCUSSION

All the Er^{3+}-doped glass samples were of transparently pink color. DSC curves of $75TeO_2$-$20ZnO$-$5K_2O$, $60TeO_2$-$15BO_{3/2}$-$20ZnO$-$5K_2O$, and $60TeO_2$-$7.5BO_{3/2}$-$7.5GeO_2$-$20ZnO$-$5K_2O$ glasses are shown in Fig. 1. Crystallization on-set temperature, T_x, and crystallization peak temperature, T_c, were significantly

increased, and glass transition temperature, T_g, was decreased with substitution of B_2O_3 and GeO_2 for TeO_2. Table 1 shows the changes of T_g, T_x, T_c and T_x - T_g with the concentration of B_2O_3 and GeO_2. The value of $T_x - T_g$ has been frequently used as a measure of thermal stability of the host glass for fiber drawing [10], [11]. It is desirable for a host glass to have a large value of $T_x - T_g$ for an optical fiber drawing. As shown in Table 1, the value of $T_x - T_g$ was increased with substitutions of B_2O_3 or GeO_2 for TeO_2, and increased further with mixed substitutions of B_2O_3 and GeO_2 compared to the separate B_2O_3 or GeO_2 substitutions. Thermal stability of tellurite glasses may be improved with the addition of SiO_2, but SiO_2 cannot use for substitution material because TeO_2–SiO_2–ZnO–K_2O glasses were spontaneously phase separated even though glass melt was quenched by a brass plate. Since B_2O_3 and GeO_2 are glass network formers having a high phonon energy, their additions into tellurite glasses can improve the glass forming ability and thus enhance the thermal stability.

Emission spectra of $75TeO_2$-$20ZnO$-$5K_2O$-$0.1Er_2O_3$, $60TeO_2$-$15GeO_2$-$20ZnO$-$5K_2O$-$0.1Er_2O_3$, and $60TeO_2$-$15BO_{3/2}$-
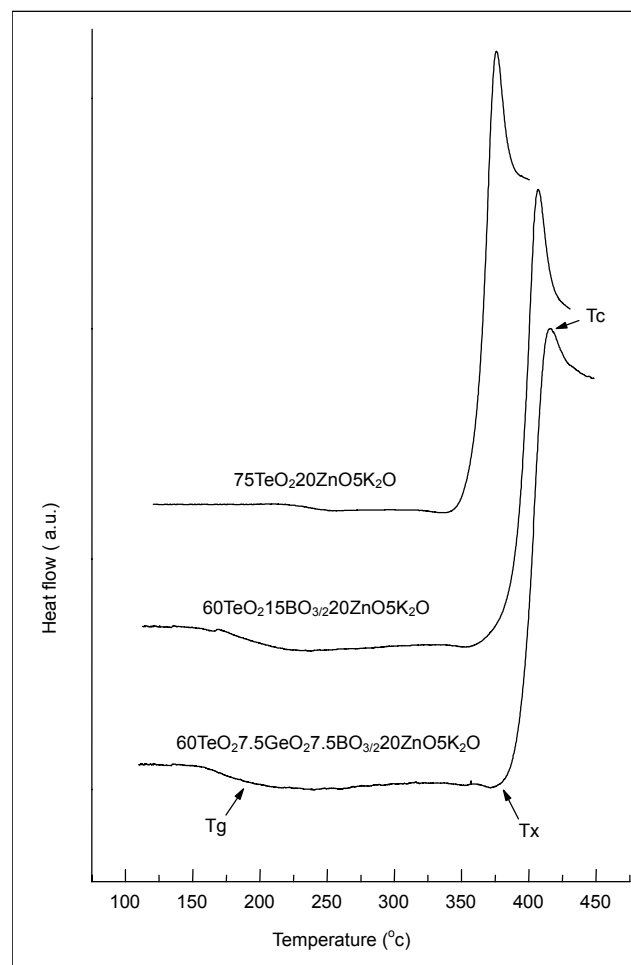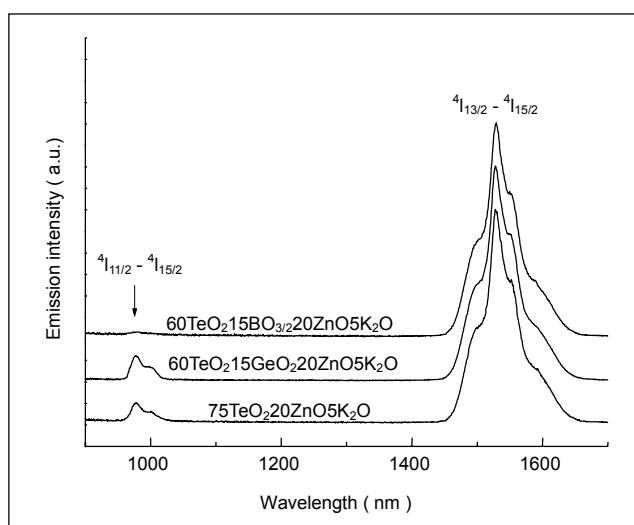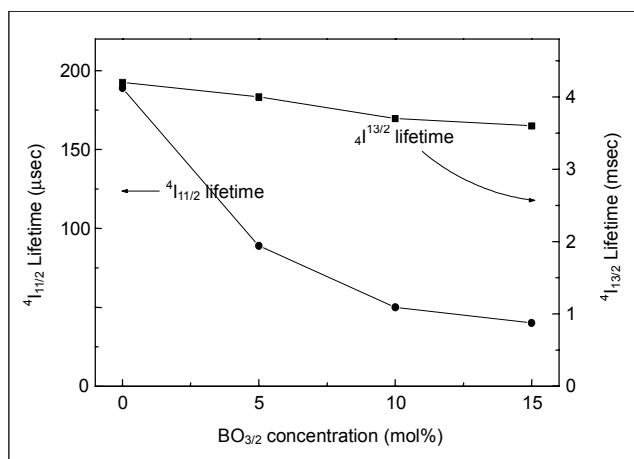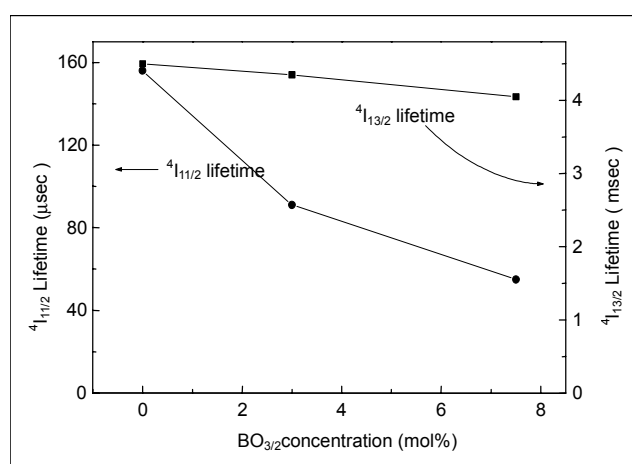

Fig. 1. DSC curves for tellurite glasses.

Table 1. T_g, T_x and T_x-T_g of tellurite glasses measured by DSC.

Composition	T_g (°C)	T_x (°C)	T_c (°C)	T_x-T_g
75TeO$_2$-20ZnO-5K$_2$O	235±5	342±2	376±2	107
70TeO$_2$-5BO$_{3/2}$-20ZnO-5K$_2$O	205±7	355±2	384±2	150
65TeO$_2$-10BO$_{3/2}$-20ZnO-5K$_2$O	200±5	360±3	392±3	160
60TeO$_2$-15BO$_{3/2}$-20ZnO-5K$_2$O	200±5	360±2	392±2	160
60TeO$_2$-15GeO$_2$-20ZnO-5K$_2$O	220±5	373±2	404±2	153
60TeO$_2$-12GeO$_2$-3BO$_{3/2}$-20ZnO-5K$_2$O	210±7	373±3	404±3	163
60TeO$_2$-7.5GeO$_2$-7.5BO$_{3/2}$-20ZnO-5K$_2$O	200±5	378±2	409±2	178

Fig. 2. Emission spectra for Er^{3+}-doped tellurite glasses.

Fig. 3. The dependence of $^4I_{11/2}$ and $^4I_{13/2}$ lifetimes on B$_2$O$_3$ concentrations in (75-x) TeO$_2$-xBO$_{3/2}$-20ZnO-5K$_2$O glasses.

Fig. 4. The dependence of $^4I_{11/2}$ and $^4I_{13/2}$ lifetimes on B$_2$O$_3$ concentrations in 60TeO$_2$-(15-x) GeO$_2$-xBO$_{3/2}$-20ZnO-5K$_2$O glasses.

20ZnO-5K$_2$O-0.1Er$_2$O$_3$ glasses are shown in Fig. 2. The GeO$_2$ substitution for TeO$_2$ hardly changed the shape of emission spectrum of Er^{3+}, but the B$_2$O$_3$ substitution almost eliminated the 980 nm emission ($^4I_{11/2} \rightarrow {}^4I_{15/2}$) peak. The B$_2O_3$ substitution was more effective than the GeO$_2$ substitution for optical quenching of $^4I_{11/2} \rightarrow {}^4I_{15/2}$ transition. Figure 3 shows the lifetime dependence of the $^4I_{11/2}$ and $^4I_{13/2}$ levels on the B$_2$O$_3$ concentration in (75-x)TeO$_2$-xBO$_{3/2}$-20ZnO-5K$_2$O glasses. The lifetime of the $^4I_{11/2}$ level was remarkably shortened as the B$_2$O$_3$ concentration increased, while that of $^4I_{13/2}$ showed a small change. Figure 4 shows the lifetime dependence of the $^4I_{11/2}$ and $^4I_{13/2}$ levels on the B$_2$O$_3$ concentration in 60TeO$_2$-(15-x)GeO$_2$-xBO$_{3/2}$-20ZnO-5K$_2$O glasses. As shown in Fig. 3 and 4, the lifetimes for $^4I_{11/2}$ and $^4I_{13/2}$ of Er^{3+} in a 75TeO$_2$-20ZnO-5K$_2$O glass were measured to be 190 μs and 4.2 ms, respectively. Those in a 60TeO$_2$-15GeO$_2$-20ZnO-5K$_2$O glass were 160 μs and 4.5 ms, and those in a 60TeO$_2$-15BO$_{3/2}$-20ZnO-5K$_2$O glass were 40 μs and 3.6 ms, respectively. The decreasing effect on the lifetime for $^4I_{11/2}$ level by the GeO$_2$ substitution was much smaller than that by the B$_2$O$_3$ substitution. The substitution of GeO$_2$ for TeO$_2$ increased the lifetime of the $^4I_{13/2}$ level, but the substitution of B$_2$O$_3$ for TeO$_2$ shortened it.

Table 2. Refractive indices and Judd-Ofelt intensity parameters of Er^{3+} in tellurite glasses.

Composition	n (1500 nm)	Ω_2 ($10^{-20}cm^2$)	Ω_4 ($10^{-20}cm^2$)	Ω_6 ($10^{-20}cm^2$)	rms (%)
75TeO$_2$-20ZnO-5K$_2$O	2.06	5.95	2.06	1.07	3.2
60TeO$_2$-15BO$_{3/2}$-20ZnO-5K$_2$O	1.97	7.33	2.60	1.19	2.9
60TeO$_2$-15GeO$_2$-20ZnO-5K$_2$O	2.00	6.98	2.52	1.10	4.2
60TeO$_2$-7.5GeO$_2$-7.5BO$_{3/2}$-20ZnO-5K$_2$O	1.98	7.15	2.60	1.19	2.9

Measured decay rate (W_m) from the excited state energy level can be expressed as

$$W_m = W_r + W_{mp} + W_{et} + W_{cr}, \qquad (1)$$

where W_r is the radiative transition rate calculated from Judd-Ofelt analysis and W_{mp}, W_{et} and W_{cr} are the rates of non-radiative transitions due to multiphonon relaxation, energy transfer, and cross relaxation, respectively [12]. Because the concentration of the Er^{3+} ion was kept low enough, W_{et} and W_{cr} can be neglected in our cases. Thus, W_m can be written as

$$W_m = \frac{1}{\tau_m} = W_r + W_{mp}. \qquad (2)$$

The Judd-Ofelt (J-O) approach for determining radiative and nonradiative transition rates of rare earth ion in glass has been widely used [7], [10], [13]. In the J-O analysis, the line strength for an electric dipole transition is given by

$$S_{ed}(aJ;bJ') = e^2 \sum_{t=2,4,6} \Omega_t \left| \left\langle f^N[\alpha SL]J \| U^{(t)} \| f^N[\alpha'S'L']J' \right\rangle \right|^2, \qquad (3)$$

where Ω_t is J-O parameter and $\left\langle \| U^{(t)} \| \right\rangle$ is doubly reduced matrix element [14], [15]. The J-O parameters are determined from absorption spectra and refractive indices. We calculated the values of Ω_2, Ω_4, and Ω_6 for our tellurite glass samples by using the procedure provided in [13]. In these calculations, the doubly reduced matrix elements from Weber [16] were used. The values of J-O parameters for the tellurite glasses are listed in Table 2. After obtaining J-O parameters, the radiative transition rate (W_r) can be determined by

$$W_r(aJ;bJ') = \frac{16\pi^3 n^2}{3h\varepsilon_0\lambda^3(2J+1)}(\chi_{ed}S_{ed} + \chi_{md}S_{md}), \qquad (4)$$

where the χ terms account for a local field correction and are given by $\chi_{ed} = (n^2+2)^2/9n$ and $\chi_{md} = n$ [16], [17]. By using (2) and (4), the multiphonon relaxation rates can be determined. The calculated radiative transition rates (W_r), measured life-times (τ_m), quantum efficiencies ($\eta = \tau_m/\tau_r$), and multiphonon relaxation rates (W_{mp}) of Er^{3+} in the tellurite glasses are listed in Table 3. It can be seen from Table 3 that the W_{mp} for $^4I_{11/2} \rightarrow$ $^4I_{13/2}$ transition was increased significantly by the B$_2$O$_3$ substitution; however, the change of that by the GeO$_2$ substitution was small. The calculations for W_{mp} of $^4I_{13/2} \rightarrow$ $^4I_{15/2}$ transitions resulted in nearly 0 in the tellurite glasses except for 60TeO$_2$-15BO$_{3/2}$-20ZnO-5K$_2$O glass.

On the other hand, an empirical rule for the multiphonon relaxation rate is written as

$$W_{mp} = W_0 \exp(-\alpha\Delta E), \qquad (5)$$

where W_0 is a positive constant depending on host glasses, ΔE is an energy gap between the excited state energy level of interest and immediately lower level [18]. It can be seen from (5) that the multiphonon relaxation rate is exponentially increased with decreasing ΔE. And α is given by

$$\alpha = \frac{1}{h\nu}\left[\ln\left(\frac{p}{g}\right) - 1\right], \qquad (6)$$

where $h\nu$ is the phonon energy coupled to rare earth ions, p is the effective number of phonons participating in the multiphonon relaxation and g is electron-phonon coupling strength [19]. Therefore, it is considered from the above (5) and (6) that the multiphonon relaxation rate is increased and the measured lifetime is decreased by increasing the phonon energy of host glasses.

B$_2$O$_3$, SiO$_2$ and GeO$_2$ are glass network formers having phonon energy higher than that of TeO$_2$. The addition of these formers into tellurite glasses increases the phonon energy of host glasses. The energy gap between $^4I_{11/2}$ and $^4I_{13/2}$ is about 3600 cm^{-1}. The highest phonon energy of borate glass, germanate glass, and tellurite glass is approximately 1400 cm^{-1}, 900

Table 3. Calculated radiative transition rates (W$_r$), measured lifetimes (τ_m), quantum efficiencies (η), and multiphonon relaxation rates (W$_{mp}$) of Er^{3+} in tellurite glasses.

glass	transition	Wr (s^{-1})	τ_m (μs)	η (%)	W$_{mp}$ (s^{-1})
1	$^4I_{13/2} \rightarrow {}^4I_{15/2}$	246	4200	103	0
	$^4I_{11/2} \rightarrow {}^4I_{13/2} , {}^4I_{15/2}$	306	190	6	4960
2	$^4I_{13/2} \rightarrow {}^4I_{15/2}$	235	3600	85	42
	$^4I_{11/2} \rightarrow {}^4I_{13/2} , {}^4I_{15/2}$	295	40	1	24700
3	$^4I_{13/2} \rightarrow {}^4I_{15/2}$	231	4500	104	0
	$^4I_{11/2} \rightarrow {}^4I_{13/2} , {}^4I_{15/2}$	289	160	5	5960
4	$^4I_{13/2} \rightarrow {}^4I_{15/2}$	233	4100	96	11
	$^4I_{11/2} \rightarrow {}^4I_{13/2} , {}^4I_{15/2}$	292	55	2	17900

* The composition of the glass 1 is 75TeO$_2$-20ZnO-5K$_2$O, the glass 2 60TeO$_2$-15BO$_{3/2}$-20ZnO-5K$_2$O, the glass 3 60TeO$_2$-15GeO$_2$-20ZnO-5K$_2$O, and the glass 4 60TeO$_2$-7.5GeO$_2$-7.5BO$_{3/2}$-20ZnO-5K$_2$O.

Table 4. σ_a, σ_e and $\sigma_e \times \tau_m$ for the Er^{3+}: $^4I_{13/2} \rightarrow {}^4I_{15/2}$ transition in the tellurite glasses at peak wavelength.

Composition	σ_a (peak λ)	σ_e (peak λ)	$\sigma_e \times \tau_m$
75TeO$_2$-20ZnO-5K$_2$O	8.55x10^{-21}cm^2 (1530nm)	8.82x10^{-21}cm^2 (1530nm)	3.70x10^{-23} cm^{2}s
60TeO$_2$-15BO$_{3/2}$-20ZnO-5K$_2$O	7.39x10^{-21}cm^2 (1534nm)	7.82x10^{-21}cm^2 (1535nm)	2.82x10^{-23} cm^{2}s
60TeO$_2$-15GeO$_2$-20ZnO-5K$_2$O	7.38x10^{-21}cm^2 (1536nm)	7.95x10^{-21}cm^2 (1537nm)	3.58x10^{-23} cm^{2}s
60TeO$_2$-7.5GeO$_2$-7.5BO$_{3/2}$-20ZnO-5K$_2$O	7.38x10^{-21}cm^2 (1534nm)	7.84x10^{-21}cm^2 (1535nm)	3.18x10^{-23} cm^{2}s

cm^{-1}, and 700 cm^{-1}, respectively [6]. Only 2 ~ 3 phonons need to be combined in borate glasses in order to bridge the energy gap between $^4I_{11/2}$ and $^4I_{13/2}$, while approximately 4 and 5 phonons need in germanate glasses and tellurite glasses, respectively. Thus, only in the case of the B$_2$O$_3$ substitution into tellurite glasses did the W_{mp} of the $^4I_{11/2} \rightarrow {}^4I_{13/2}$ transition increase. On the other hand, the energy gap between $^4I_{13/2}$ and $^4I_{15/2}$ is about 6500 cm^{-1}, and thus the multiphonon relaxation rate is very small. The lifetime of the $^4I_{13/2}$ level is hardly affected by the change of the phonon energy in host glasses. Therefore, the decreasing effect on the $^4I_{13/2}$ lifetime by the B$_2$O$_3$ substitution was small. In the case of the GeO$_2$ substitution, the measured lifetime of the $^4I_{13/2}$ level increased. This is considered to result from the increase of intrinsic radiative lifetime ($\tau_r = 1/W_r$) with the GeO$_2$ substitution as shown in Table 3. The intrinsic radiative lifetime is increased by lowering the refractive indices [20], and the GeO$_2$ substitution reduced the refractive indices as shown in Table 2.

The peak wavelength of the emission cross-section for the $^4I_{13/2} \rightarrow {}^4I_{15/2}$ transition was shifted to a long wavelength side by the B$_2$O$_3$ and GeO$_2$ substitutions as shown in Table 4. The spectral gain profile of EDFA strongly depends on the difference spectrum of σ_e - σ_a [20]. The peak wavelength of σ_e - σ_a was also shifted to a long wavelength side by the B$_2$O$_3$ and GeO$_2$ substitution as shown in Fig. 5. Thus, the corresponding spectral gain profile is expected to shift to a long wavelength region.

The fluorescence efficiency of an active ion in solids can be expressed in terms of a combination of various spectroscopic parameters such as absorption and emission cross-sections, excited state lifetimes, transition probabilities, and concentration of dopant ions [21]. The large emission cross-section and the long lifetime of the excited state energy level make the rare earth doped materials promising materials for fiber amplifier applications [22], [23]. The absorption and emission cross-sections of Er^{3+}: $^4I_{13/2} - {}^4I_{15/2}$ in 75TeO$_2$-20ZnO-5K$_2$O and 60TeO$_2$-7.5 GeO$_2$-7.5BO$_{3/2}$-20ZnO-5K$_2$O glasses are also shown in Fig. 5. The absorption cross-sections were determined from absorption spectrum, and the emission cross-sections were calculated by McCumber theory [24]. According to McCumber theory, the emission cross-sections and the absorption cross-sections are related by
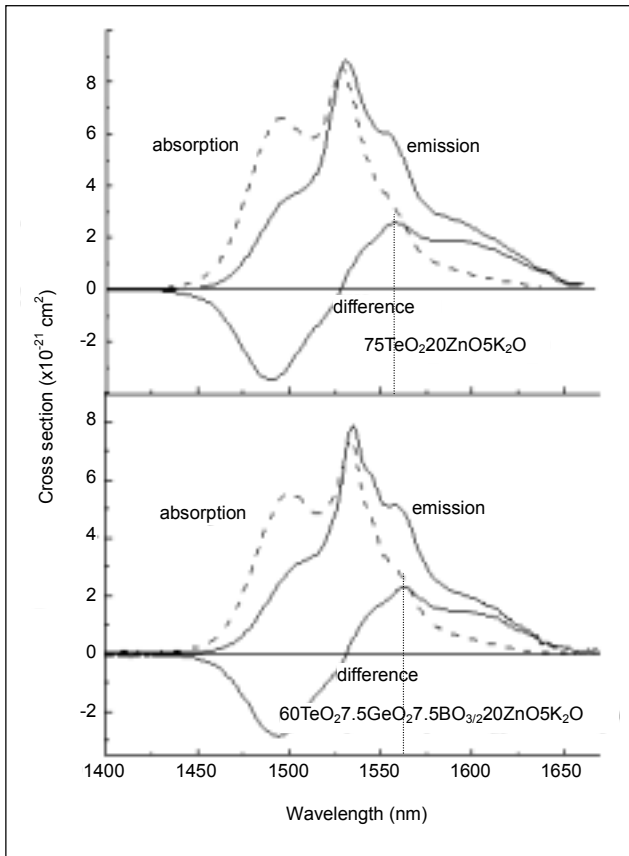
Fig. 5. The spectra of absorption cross-section (σ_a), emission cross-section (σ_e), and $\sigma_e - \sigma_a$ for the Er^{3+} : $^4I_{13/2} \rightarrow {}^4I_{15/2}$ transition in the tellurite glasses.

$$\sigma_e(\nu) = \sigma_a(\nu)\exp[(\varepsilon-h\nu)/kT], \qquad (7)$$

where ε is the temperature dependent excitation energy, h is the Plank constant, k is the Boltzmann constant, and T is the temperature. The value of ε was determined by using the procedure provided in [25]. The emission cross-sections decreased with the B_2O_3 and GeO_2 substitutions for TeO_2 as shown in Table 4. The decreasing effect on the emission cross-section by the GeO_2 substitution was smaller than that by the B_2O_3 substitution. The B_2O_3 and GeO_2 substitutions for TeO_2 also lowered refractive indices of host glasses. The emission cross-section is expected to be decreased with lowering the refractive index of a host glass, because the stimulated emission cross-section owing to the electric dipole-moment transition of rare earth ions is increased as the refractive index of a host glass is raised [$\sigma \sim (n^2+2)^2/n$] [26]. Often the value of σ_e (emission cross-section) $\times$ τ_m (measured lifetime) is used as a material parameter of estimation for fiber amplifier applications [27], [28]. The value of $\sigma_e \times \tau_m$ for the Er^{3+}: $^4I_{13/2} \rightarrow {}^4I_{15/2}$ transition in the $60TeO_2$-$15BO_{3/2}$-$20ZnO$-$5K_2O$ glass was reduced by about 24% compared to that in the $75TeO_2$-$20ZnO$-$5K_2O$ glass, while that of

the $60TeO_2$-$15GeO_2$-$20ZnO$-$5K_2O$ glass was reduced merely by 3%. The GeO_2 substitution reduced the emission cross-section, but extended the lifetime. Thus, the GeO_2 substitution scarcely changed the value of $\sigma_e \times \tau_m$ in Er^{3+}-doped tellurite glasses. However, only the GeO_2 substitution was not enough to raise the multiphonon relaxation rate of $^4I_{11/2} \rightarrow {}^4I_{13/2}$ transition as shown in Table 3. Therefore, TeO_2-GeO_2-B_2O_3-MO-R_2O glass system is expected to be a suitable host glass for the tellurite-based erbium-doped fiber amplifier material with a high 980 nm pump efficiency, where M indicates a divalent metal such as Zn and Ba and R indicates an alkali metal.

IV. CONCLUSIONS

The substitutions of B_2O_3 and GeO_2 improved the thermal stability of tellurite glasses. The substitution of B_2O_3 into tellurite glasses significantly raised the multiphonon relaxation rate of Er^{3+}: $^4I_{11/2} \rightarrow {}^4I_{13/2}$, which was thus expected to enhance the 980 nm pumping efficiency in T-EDFA. However, the B_2O_3 substitution caused the reduction of the $^4I_{13/2}$ lifetime and the emission cross-section for Er^{3+}: $^4I_{13/2} \rightarrow {}^4I_{15/2}$. On the other hand, the GeO_2 substitution into the tellurite glasses extended the $^4I_{13/2}$ lifetime and slightly reduced the emission cross-section, but the increasing effect on the multiphonon relaxation rate for the $^4I_{11/2} \rightarrow {}^4I_{13/2}$ transition was small. Therefore, TeO_2-GeO_2-B_2O_3–MO-R_2O glass system is expected to be a suitable host glass for the tellurite-based erbium-doped fiber amplifier material with a high 980 nm pump efficiency.

REFERENCES

[1] A. Mori, Y. Ohishi, M. Yamada, H. Ono, Y. Nishida, K. Oikawa, and S. Sudo, "1.5 μm Broadband Amplification by Tellurite-Based EDFAs," *Technical Digest of Conf. Optical Fibe-Comm.1997* (OFC'97), Feb. 16-21, 1997, Dallas, Texas, US, PD1

[2] Y. Ohishi, A. Mori, M. Yamada, H. Ono, Y. Nishida, and K. Oikawa, "Gain Characteristics of Tellurite-Based Erbium-Doped Fiber Amplifiers for 1.5-μm Broadband Amplification," *Opt. Lett.*, vol. 23, no. 4, 1998, p.274.

[3] W.J. Miniscalco, "Erbium-Doped Glasses for Fiber Amplifiers at 1500 nm," *J. Lightwave Technol.*, vol. 9, 1991, p.234.

[4] T. Nakai, Y. Noda, T. Tani, Y. Mimura, T. Sudo, and S. Ohno, "980 nm-Pumped Er-Doped Tellurite-Based Fiber Amplifier," *OSA TOPS*, vol. 25, 1998, p.82.

[5] M.P. Hehlen, N.J. Cockroft, T.R. Gosnell, and A.J. Bruce, "Spectroscopic Properties of Er^{3+}- and Yb^{3+}-Doped Soda-Lime Silicate and Aluminosilicate Glasses," *Phys. Rev. B*, vol. 56, 1997, p.9302.

[6] R. Reisfeld and C.K. Jorgensen, in *Handbook of Physics and Chemistry of Rare Earths*, edited by K.A. Gschneidner, Jr. and L. Eyring, Elsevier Science Publishers B.V., 1987.

[7] X. Zou and T. Izumitani, "Spectroscopic Properties of Er^{3+}- and

Yb^{3+}-Doped Soda-Lime Silicate and Aluminosilicate Glasses," *J. Non-Cryst. Solids*, vol. 162,1993, p.68.

[8] R.S. Quimby, "Output Saturation in a 980 nm Pumped Erbium-Doped Fiber Amplifier," *Appl. Opt.*, vol. 30, 1991, p.2546.

[9] Y.G. Choi, D.S. Lim, K.H. Kim, D.H. Cho, and H.K. Lee, "Enhanced $^4I_{11/2} \rightarrow ^4I_{13/2}$ Transition Rate in Er^{3+}/Ce^{3+}-Codoped Tellurite Glasses," *Electron. Lett.* vol. 35, no. 20, 1999, p.1765.

[10] J.S. Wang, E.M. Vogel, and E. Snitzer, "Tellurite Glass: a New Candidate for Fiber Devices," *Optical Materials*, vol. 3, 1994, p.187.

[11] M.G. Drexhage, O.H. El-Bayoumi, C.T. Moynihan, A.J. Bruce, K.H. Chung, D.L. Gavin, and J.T. Loretz, "Preparation and Properties of Heavy-Metal Fluoride Glasses Containing Ytterbium or Lutetium," *J. Am. Ceram. Soc*. vol. 65, 1982, p.168.

[12] H. Toratani, T. Izumitani, and H. Kuroda, "Compositional Dependence of Nonradiative Decay Rate in Nd Laser Glasses," *J. Non-Cryst. Solids*, vol. 52, 1982, p.303.

[13] Z. Pan and S.H. Morgan, "Optical Transitions of Er^{3+} in Lead-Tellurium-Germanate Glasses," *J. Lumin.*, vol. 75, 1997, p.301.

[14] B.R. Judd, "Optical Absorption Intensities of Rare Earth Ions," *Phys. Rev.*, vol. 127, 1962, p.750.

[15] G.S. Ofelt, "Intensities of Crystal Spectra of Rare Earth Ions," *J. Chem. Phys.*, vol. 37, 1962, p.511.

[16] M.J. Weber, "Probabilities for Radiative and Nonradiative Decay of Er^{3+} in LaF3," *Phys. Rev.*, vol. 157, 1967, p.262.

[17] M.D. Shinn, W.A. Silbley, M.G. Drexhage, and R.N. Brown, "Optical Transitions of Er^{3+} Ions in Fluorozirconate Glass," *Phys. Rev. B*, vol. 27, 1983, p.6635.

[18] M.J. Weber, "Multiphonon Relaxation of Rare-Earth Ions in Yttrium Orthoaluminate," *Phys Rev. B*, vol. 8, no.1, 1973, p.54.

[19] T. Miyakawa and D.L. Dexter, "Photon Sidebands, Multiphonon Relaxation of Excited States, and Phonon-Assisted Energy Transfer between Ions in Solids," *Phys. Rev. B*, vol. 1, 1970, p.2961.

[20] Y. Ohishi, *Optical Fiber Amplifiers: Materials, Devices, and Applications*, edited by S. Sudo, Artech House, 1997.

[21] A.A. Kaminski, *Laser Crystals: Their Physics and Properties*, Springer, Berlin, 1975.

[22] E. Desurvire, *Erbium-Doped Fiber Amplifiers: Principles and Applications*, John Wiley & Sons, 1994.

[23] K. Wei, D.P. Machewirth, J. Wenzel, E. Snitzer, and G.H. Sigel Jr., "Pr^{3+}-Doped Ge-Ga-S Glasses for 1.3 μm Optical Fiber Amplifiers," *J. Non-Cryst. Solids*, vol. 182, 1995, p.257.

[24] D.E. Mc Cumber, "Theory of Phonon-Terminated Optical Masers," *Phys. Rev. A*, vol. 134, 1964, p.299.

[25] W.J. Miniscalco and R.S. Quimby, "General Procedure for the Analysis of Er^{3+} Cross-Sections," *Opt. Lett.*, vol. 16, 1991, p.258.

[26] R. Reisfeld and C.K. Jorgensen, *Laser and Excited States of Rare Earths*, Springer-Verlag, New York, 1997.

[27] D.R. Simons, A.J. Faber, and H. de Waal, "Pr^{3+}-Doped GeSx-Based Glasses for Fiber Amplifiers at 1.3 μm," *Opt. Lett.*, vol. 20, no. 5, 1995, p. 468.

[28] Yong Gyu Choi, Bong Je Park, Kyong Hon Kim, and Jong Heo, "Pr^{3+}- and Pr^{3+}/Er^{3+}-Doped Selenide Glasses for Potential 1.6 μm Optical Amplifier Materials," *ETRI J.*, vol. 23, no. 3, 2001, p. 97.

Doo Hee Cho received the Ph.D. degree in materials chemistry from Kyoto University in 1996. He worked in area of the glass fiber manufacturing, float glass manufacturing, and LOW-E coating on float glass at the Glass Research Center, Keumkang Chemical Co. during the period from 1996 to 1998. Since joining Telecommunication Basic Research Laboratory of ETRI in 1998, he has been involved in specialty fiber material and device research. His major research interests include non-silica glasses for fiber amplifier and glass planar waveguide devices.

Yong Gyu Choi received the B.S. degree from KAIST in 1991. Then, he moved to POSTECH where he earned his M.S. and Ph.D. degrees in 1994 and in 1998, respectively. During the period of 1994 to 1998, his works were focused on processing and characterizing amorphous materials doped with rare-earth elements. Since joining Telecommunication Basic Research Laboratory of ETRI in 1998, he has been involved in research in optical materials and devices for advanced optical communications. His current research interests include not only development of new optical fiber amplifiers and nonlinear fiber devices but also spectroscopic analysis of optical materials especially with X-ray absorption spectroscopy using synchrotron radiation.

Kyong Hon Kim received the B.S. degree from Kyungpook National University in 1979 and the Ph.D. degree from State University of New York at Buffalo, USA in 1986, both in physics. During the period of 1986 to 1989, he worked in the area of dye and solid-state lasers and their application in space science at NASA Langley Research Center, and served as a Research Assistant Professor in Hampton University, Virginia, USA. Since he joined Basic Research Laboratory of ETRI in 1989, he has been involved in fiber-optic device research for advanced optical communications. He is now in charge of technical management of optical communication device research activities based on fiber, semiconductor, and polymer materials.